Probing Photophysical Processes in Individual Multichromophoric Dendrimers by Single-Molecule Spectroscopy

Johan Hofkens,[†] **Michael Maus,**[†] **Thomas Gensch,**[†] **Tom Vosch,**[†] **Mircea Cotlet,**[†] **Fabian Köhn,**[†] **Andreas Herrmann,**[‡] **Klaus Müllen,**[‡] **and Frans De Schryver*,**[†]

Contribution from the Department of Chemistry, Katholieke Universiteit Leuven, Celestijnenlaan 200 F, BE-3001 Heverlee-Leuven, Belgium, and Max-Planck-Institute für Polymerforschung, Ackermannweg 10, 55128 Mainz, Germany

Abstract: Individual multichromophoric dendrimer molecules, bearing eight perylenecarboximide chromophores at the rim, immobilized in a thin polyvinylbutyral (PVB) film were studied by far-field fluorescence microscopy. Fluorescence intensity trajectories as a function of time (transients), spectra, and decay traces were recorded separately or simultaneously. For comparison, similar measurements have been performed on a model compound containing one perylenecarboximide chromophore. Collective on/off jumps of the fluorescence intensity were observed for single dendrimer molecules, resembling previously reported collective jumps for the emission of single light-harvesting antenna systems. Spectra and decays of both non-interacting and dimer-like interacting chromophoric sites could be distinguished within an individual dendrimer. Transitions between the different spectral forms and decay times, observed for a single molecule, underline the dynamic character of the interactions among the chromophores. Evidence for a stepwise bleaching process of the multichromophoric system was found. Furthermore, the single-molecule data incontestably prove the assumptions stated in the ensemble model.

Introduction

Dendrimers are a class of macromolecules with a perfectly controllable branched structure. The molecular architecture of the dendrimer consists of three structural units, the core, a hyperbranched shell, and an external surface. The individual layers around the core are designated as generations. A lot of effort has been put into the development of different methodologies for the synthesis of new dendrimers.[1,2] Dendrimers have been shown to possess unusual physical and chemical properties which differ significantly from that of linear polymers.[3] New applications, based on these structure-controlled architectures, have made dendrimers the object of wide interdisciplinary interest.[4,5] By using a fluorescent chromophore as the core of a dendrimer, one can apply fluorescence spectroscopy to study structural aspects and conformational mobility of dendrimers in solution.[6−8] At the same time, the dendritic shell provides a unique nanometer-size environment for the spatial isolation of the chromophore, making them interesting objects for investigations by modern scanning probe microscopy techniques as well as for single-molecule spectroscopy (SMS).[9,10] Fluorescent chromophores can also be attached to the external surface of the dendrimer. Thus, dendrimer synthesis serves as a way to obtain a well-defined number of chromophores in a confined volume element. Not only can the number of chromophores be easily controlled, but also the interactions among the chromophores can be governed by changing the structure of the branches to which the chromophores are attached or by attaching the branches to different cores. The chromophores in each branch of the dendrimer readily allow the interactions of the branches, conformational distortions, as well as excitation energy transfer or electron transfer among the chromophores to be probed.[11−15] One of the interesting questions that might be addressed with SMS of multichromophoric dendritic systems is whether there is a transition from single-molecule behavior (discrete on/off jumps in fluorescence intensity of one chromophore) to ensemble behavior (exponential bleaching of the fluorescence intensity). The system discussed in this contribution, although containing eight chromophores, still behaves as a single emitting quantum system, showing collective on/off behavior similar to the on/off behavior reported for single

† Katholieke Universiteit Leuven.
‡ Max-Planck-Institut für Polymerforschung.
(1) Newkome, G. R.; Moorefield, C. N.; Vögtle, F. *Dendritic molecules: concepts, synthesis, perspectives*; Weinheim, VCH: 1996.
(2) Kim, Y.; Zimmerman, S. C. *Curr. Opin. Chem. Biol.* **1998**, *2*, 733−742.
(3) Frechet, J. M. J.; Hawker, C. J.; Gitsov, I.; Leon, J. W. *J. Macromol. Sci. Pure Appl. Chem.* **1996**, *A33*, 1399−1425.
(4) Matthews, O. A.; Shipway, A. N.; Stoddart, J. F. *Prog. Polym. Sci.* **1998**, *23*, 1−56.
(5) Narayanan, V. V.; Newkome, G. R. In *Topics In Current Chemistry*; Springer-Verlag: Berlin/Heidelberg, 1998; pp 19−77.
(6) De Backer, S.; Prinzie, Y.; Verheijen, W.; Smet, M.; Desmedt, K.; Dehaen, W.; De Schryver, F. C. *J. Phys. Chem. A* **1998**, *102*, 5451−5455.
(7) Pollak, K. W.; Leon, J. W.; Frechet, J. M. J.; Maskus, M.; Abruna, H. D. *Chem. Mater.* **1998**, *10*, 30−38.
(8) Matos, M. S.; Hofkens, J.; Verheijen, W.; De Schryver, F. C.; Hecht, S.; Pollak, K. W.; Frechet, J. M. J.; Forier, B.; Dehaen, W. *Macromolecules* **2000**, *33*, 2967−2973.

(9) Hofkens, J.; Verheijen, W.; Shukla, R.; Dehaen, W.; De Schryver, F. C. *Macromolecules* **1998**, *31*, 4493−4497.
(10) Veerman, J. A.; Levi, S. A.; van Veggel, F. C. J. M.; Reinhoudt, D. N.; van Hulst, N. F. *J. Phys. Chem. A* **1999**, *103*, 11264−11270.
(11) Devadoss, C.; Bharathi, P.; Moore, J. S. *J. Am. Chem. Soc.* **1996**, *118*, 9635−9644.
(12) Kopelman, R.; Shortreed, M.; Shi, Z. Y.; Tan, W. H.; Xu, Z. F.; Moore, J. S.; BarHaim, A.; Klafter, J. *Phys. Rev. Lett.* **1997**, *78*, 1239−1242.
(13) Adronov, A.; Gilat, S. L.; Frechet, J. M. J.; Ohta, K.; Neuwahl, F. V. R.; Fleming, G. R. *J. Am. Chem. Soc.* **2000**, *122*, 1175−1185.
(14) Gilat, S. L.; Adronov, A.; Frechet, J. M. J. *Angew. Chem., Int. Ed.* **1999**, *38*, 1422−1427.
(15) Balzani, V.; Campagna, S.; Denti, G.; Juris, A.; Serroni, S.; Venturi, M. *Acc. Chem. Res.* **1998**, *31*, 26−34.

molecules containing one chromophore.[16-18] On the other hand, it is well known that small beads labeled with chromophores show an exponential photobleaching behavior.[19] As dendritic systems make it possible to change, in a controlled way, the amount of chromophores in a confined space as well as the interactions between chromophores and the interchromophoric distances, study of these systems might lead to the observation of and insight into the transition from the single-molecule regime to the ensemble regime.

Collective effects, as seen for the multichromoporic dendrimer, were also observed for natural light-harvesting antenna systems and a multichromophoric polymer system.[20-22] The former systems possess a well-defined number of chromophores that are arranged in a more or less ordered fashion by the surrounding protein. It is believed that these collective effects are related to energy-transfer processes occurring in the multichromophoric antenna system. Moreover, in a recent publication the role of disorder (due to slow and fast fluctuations in the surrounding protein) on the energy-transfer process of antenna systems was emphasized.[23] It has been shown that SMS is an excellent technique for investigating the spatial, conformational, and temporal inhomogeneity of populations.[24,25] Therefore, we believe that SMS studies of multichromophoric dendrimer systems make it possible to investigate fundamental aspects of energy-transfer processes that are relevant for a number of multichromophoric systems, including photosynthetic complexes and conjugated polymers.[21,22,26-31]

Recently, a new type of dendrimer consisting of hexaphenylbenzene building blocks with strongly twisted benzene units was described.[32-34] The important feature of the easily soluble 3D polyphenylene dendrimers is the relatively high shape persistence.[35] Furthermore, due to the out-of-plane twist of the phenyl units with respect to one another, the core does not absorb at wavelengths of interest (above 450 nm). The new synthetic approach allows the attachment of chromophores to the branched polyphenylene molecule. As a chromophore, perylenecarboximide was introduced because of its photostability, its absorption wavelength (around 500 nm), its high absorption coefficient (38 000 M^{-1} cm^{-1} at 490 nm), and its high fluorescence quantum yield ($\phi_f = 0.95$). The polyphenylene core does not absorb at the excitation wavelengths of interest (above 450 nm).

Stationary fluorescence measurements, picosecond time-resolved single-photon timing (SPT) and femtosecond upconversion (UC) measurements as well as femtosecond transient absorption (TA) measurements in solution were performed on **g2** and compared to those on a model compound **g0** (see Figure 1).[36-39] On the basis of these ensemble measurements, a model has been proposed to explain the complex photophysical behavior of **g2**. A simplified photophysical scheme is depicted in Figure 2. The decay time of around 4 ns (SPT) is assigned to originate from non-interacting chromophores in the dendrimer and is in good agreement with the decay time of the model compound in solution. The 8-ns (SPT) component is assigned to the bathochromically shifted emission of excimer-like interacting chromophores. The fast decay components, ranging from subpicosecond (UC, TA) to several hundreds of picoseconds (SPT, UC), are attributed to vibrational relaxation and energy-transfer processes, respectively.

In this contribution, we investigate **g2** at the single-molecule level. Fluorescence transients, spectra, and decays, either individually or combined, were measured as well as polarized fluorescence transients under different excitation conditions (circular and linear polarized excitation with fixed and rotating excitation polarization direction; the latter is named modulated polarization). The results obtained for **g2** are compared to the values obtained for the model compound **g0**. It will be shown that the processes suggested in Figure 2 indeed can be found back at the single-molecule level and that the study corroborates and deepens our understanding of the photophysical processes occurring in the dendrimer.

Experimental Section

A detailed description of the synthesis of **g2** and **g0** was reported previously.[32,33,40,41]

Absorption spectra were measured on a Perkin-Elmer Lambda-6. Fluorescence spectra were recorded on a SPEX Fluorolog 1680. Information on single-photon timing (SPT) setup, the femtosecond transient absorption setup, and on the setup for upconversion measurements is published elsewhere.[37-39]

Samples for the single-molecule measurements were prepared by spin-coating solutions of **g2** and **g0** (5×10^{-10} M) in chloroform containing 3 mg/mL polyvinylbutyral (PVB) on a cover glass at 4000 rpm to yield thin (20-40 nm as measured by AFM) polymer films containing on average 0.2 molecules/μm^2. The sample preparation included careful cleaning of the glassware used for sample preparation

(16) Weston, K. D.; Buratto, S. K. *J. Phys. Chem. A* **1998**, *102*, 3635-3638.

(17) Veerman, J. A.; Garcia, P. M.; Kuipers, L.; van Hulst, N. F. *Phys. Rev. Lett.* **1999**, *83*, 2155-2158.

(18) Dickson, R. M.; Cubitt, A. B.; Tsien, R. Y.; Moerner, W. E. *Nature* **1997**, *388*, 355-358.

(19) Gensch, T.; Hofkens, J.; van Stam, J.; Faes, H.; Creutz, S.; Tsuda, K.; Jerome, R.; Masuhara, H.; De Schryver, F. C. *J. Phys. Chem. B* **1998**, *102*, 8440-8451.

(20) Bopp, M. A.; Jia, Y. W.; Li, L. Q.; Cogdell, R. J.; Hochstrasser, R. M. *Proc. Natl. Acad. Sci. U.S.A.* **1997**, *94*, 10630-10635.

(21) Bopp, M. A.; Sytnik, A.; Howard, T. D.; Cogdell, R. J.; Hochstrasser, R. M. *Proc. Natl. Acad. Sci. U.S.A.* **1999**, *96*, 11271-11276.

(22) VandenBout, D. A.; Yip, W. T.; Hu, D. H.; Fu, D. K.; Swager, T. M.; Barbara, P. F. *Science* **1997**, *277*, 1074-1077.

(23) Scholes, G. D.; Fleming, G. R. *J. Phys. Chem. B* **2000**, *104*, 1854-1868.

(24) Weiss, S. *Science* **1999**, *283*, 1676-1683.

(25) Moerner, W. E.; Orrit, M. *Science* **1999**, *283*, 1670-1676.

(26) Ying, L. M.; Xie, X. S. *J. Phys. Chem. B* **1998**, *102*, 10399-10409.

(27) van Oijen, A. M.; Ketelaars, M.; Köhler, J.; Aartsma, T. J.; Schmidt, J. *Science* **1999**, *285*, 400-402.

(28) van Oijen, A. M.; Ketelaars, M.; Köhler, J.; Aartsma, T. J.; Schmidt, J. *Chem. Phys.* **1999**, *247*, 53-60.

(29) van Oijen, A. M.; Ketelaars, M.; Köhler, J.; Aartsma, T. J.; Schmidt, J. *J. Phys. Chem. B* **1998**, *102*, 9363-9366.

(30) Wu, M.; Goodwin, P. M.; Ambrose, W. P.; Keller, R. A. *J. Phys. Chem.* **2000**, *100*, 17406-17409.

(31) Tietz, C.; Daum, R.; Drabenstedt, A.; Schuster, J.; Fleury, L.; Gruber, A.; Wachtrup, J.; von Borczyskowski, C. *Chem. Phys. Lett.* **1998**, *282*, 164-170.

(32) Morgenroth, F.; Müllen, K. *Tetrahedron* **1997**, *53*, 15349-15366.

(33) Morgenroth, F.; Berresheim, A. J.; Wagner, M.; Müllen, K. *Chem. Commun.* **1998**, 1139-1140.

(34) Morgenroth, F.; Kubel, C.; Muller, M.; Wiesler, U. M.; Berresheim, A. J.; Wagner, M.; Müllen, K. *Carbon* **1998**, *36*, 833-837.

(35) Zhang, H.; Grim, P. C. M.; Foubert, P.; Vosch, T.; Vanoppen, P.; Wiesler, U. M.; Berresheim, A. J.; Müllen, K.; De Schryver, F. C. *Langmuir*, in press.

(36) Gensch, T.; Hofkens, J.; Herrmann, A.; Tsuda, K.; Verheijen, W.; Vosch, T.; Christ, T.; Basché, T.; Müllen, K.; De Schryver, F. C. *Angew. Chem., Int. Ed.* **1999**, *38*, 3752-3756.

(37) Hofkens, J.; Latterini, L.; De Belder, G.; Gensch, T.; Maus, M.; Vosch, T.; Karni, Y.; Schweitzer, G.; Herrmann, A.; Müllen, K.; De Schryver, F. C. *Chem. Phys. Lett.* **1999**, *304*, 1-9.

(38) Karni, Y.; Jordens, S.; De Belder, G.; Hofkens, J.; Schweitzer, G.; De Schryver, F. C.; Herrmann, A.; Müllen, K. *J. Phys. Chem. B* **1999**, *103*, 9378-9381.

(39) Karni, Y.; Jordens S.; De Belder G.; Schweitzer, G.; Hofkens, J.; Gensch, T.; Maus, M.; Herrmann, A.; Müllen, K.; De Schryver, F. C. *Chem. Phys. Lett.* **1999**, *310*, 73-78.

(40) Morgenroth, F.; Kubel, C.; Müllen, K. *J. Mater. Chem.* **1997**, *7*, 1207-1211.

(41) Muller, M.; Kubel, C.; Morgenroth, F.; Iyer, V. S.; Müllen, K. *Carbon* **1998**, *36*, 827-831.
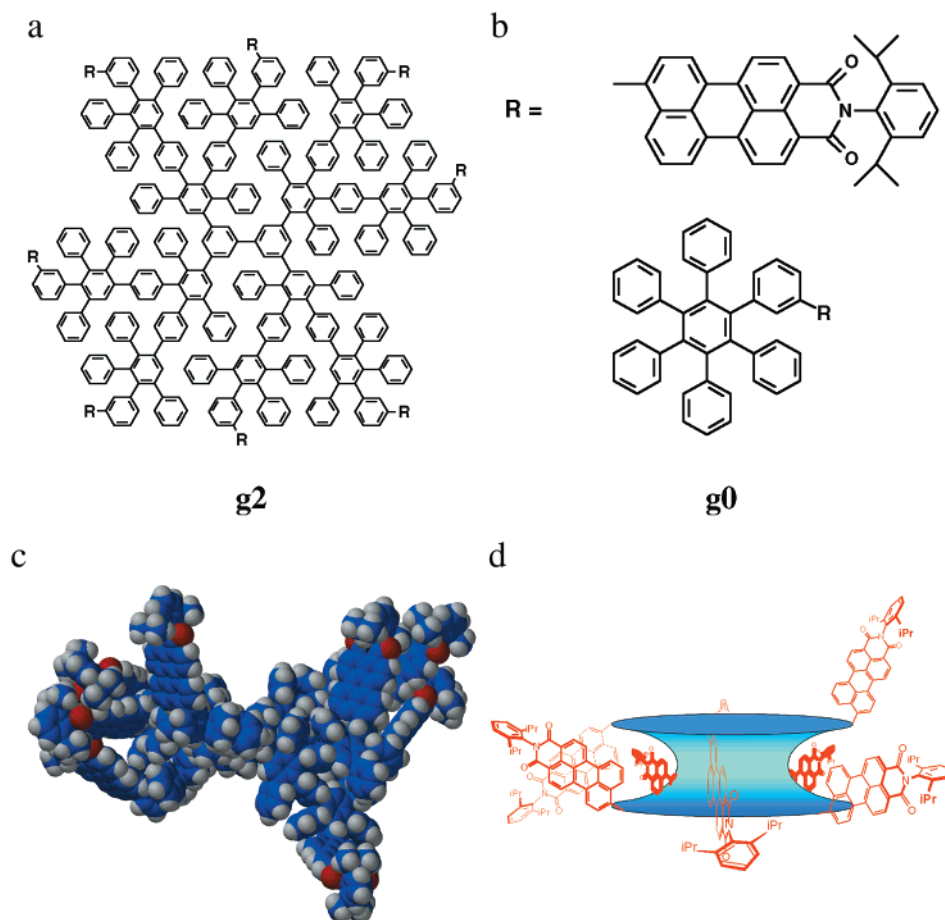
Figure 1. (a, b) Structures of the second-generation dendrimer (**g2**) and the model compound (**g0**). (c) Molecular model of **g2** as obtained from a force field minimization calculation (Merck force field, Spartan). (d) Schematic drawing of the dendrimer molecule, showing the conelike shape of the core and inhomogeneous distribution of the chromophores at the rim. The presence of isolated chromophores and interacting chromophores within one dendrimer molecule is depicted.
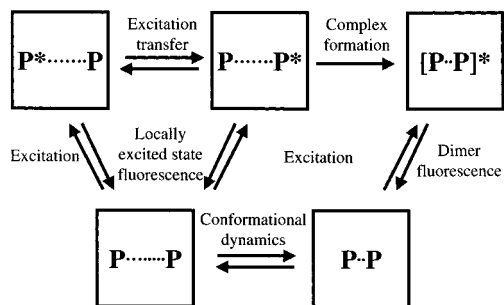
Figure 2. Simplified scheme summarizing the photophysical properties of **g2** in solution. Both isolated and interacting chromophoric sites exist in equilibrium in the ground state. In the exited state, energy transfer is possible (seen as the 1−350-ps component in the decays). The decay time associated with fluorescence of isolated chromophoric sites is 4 ns, and the decay time associated with emission from interacting chromophoric sites is 8 ns.

as well as a subsequent cleaning of the cover glasses by sonication in acetone, sodium hydroxide (10%), and MilliQ water.

The fluorescence of single molecules was detected using a confocal microscope (Diaphot 200, Nikon) with an oil immersion lens (NA 1.4) equipped with an avalanche photodiode (APD) in single-photon-counting mode (SPCM AQ15, EG&G) as the detector. Suitable filters were placed in the detection path to suppress remaining excitation light. The fluorescence intensity transients were measured with a dwell time of 5 or 10 ms. Excitation sources were an argon ion laser for 488 nm (Spectra Physics Stabilite 2017) and a helium−neon (HeNe) laser (Melles Griot 05-LGR-193) for 543 nm. The fluorescence spectra were measured with a liquid-nitrogen-cooled, back-illuminated CCD camera

(LN/CCD-512SB, Princeton Instruments) coupled to a 150-mm poly-chromator (SpectraPro 150, Acton Research Cooperation) using 5-, 8-, or 10-s integration time. The recorded spectra were corrected for the background, the response of the CCD camera, and the optics used. Determination of the peak position of each spectrum was done by calculating the first and second derivatives. The resulting accuracy is around ±1 nm. For the time-resolved measurements, the signals from the APD were collected in a time-correlated single-photon-counting (TCSPC) PC card (SPC 430, Picoquant GmbH) together with the trigger signal to record the fluorescence decays of the single molecule in steps of 1−10 s. The decays were fitted with the least-squares (LS) method.[42] The quality of the fits has been judged from the values of the reduced χ^2 (<1.2) and Z_χ^2 as well as from the residuals and the autocorrelation function. For the combined measurements (transients, spectra, and decays) the fluorescence signal of the single molecule under investigation was split with a hybrid beam splitter cube (Newport 05BC17MB.1), guiding 50% of the light to the CCD camera and 50% to the APD. Polarization measurements were performed by splitting the signal with a polarizing beam splitter cube (Newport 05FC16PB.3) and detecting s- and p-polarized components of the fluorescence light with two independent detectors. Modulation of the excitation was obtained by passing linear polarized laser light through a $\lambda/2$ plate rotating with a stable frequency. More details on the experimental setup will be published elsewhere.[43]

(42) Maus, M.; Cotlet, M.; Hofkens, J.; Gensch, T.; De Schryver, F. C.; Schaffer, J.; Seidel, C. A. M. Submitted.

(43) Maus, M.; Hofkens, J.; Gensch, T.; Cotlet, M.; De Schryver, F. C. In preparation.
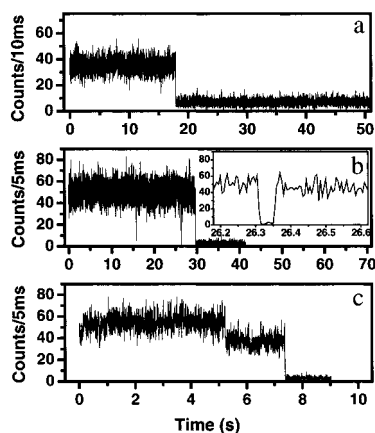
Figure 3. Transients of the model compound **g0** excited at 488 nm (intensity of 350 W/cm^2 at the sample) in a 30-nm thin PVB film. (a) 60% of the transients show a one-step photobleaching behavior and no other features. (b) 35% of the transients show one or more off periods (intensity drops to the background level). The inset is a zoom of the second off period in the depicted transient. The off time in this case is 35 ms. (c) 5% of the transients of **g0** show different intensity levels.
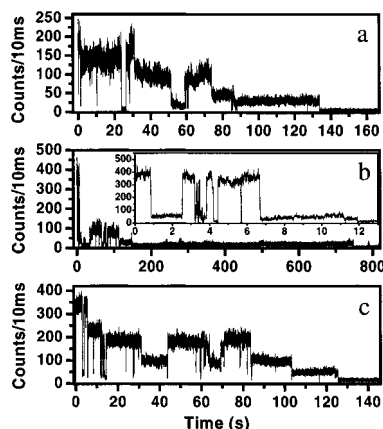
Figure 4. Transients of the dendrimer **g2** excited at 488 nm (intensity of 350 W/cm^2 at the sample) in a 30-nm thin PVB film (a, b). (a) Transient recorded with linear polarized excitation light. Several off periods as well as levels can be seen in the transient. (b) Transient recorded with circular polarized excitation light, hence sampling all eight chromophores in the dendrimer. The inset is a zoom in the first high level of the transient. Both low levels and off levels of different duration can be seen. The transient shows a long duration low level (500 s) before it finally photobleaches. (c) Transient recorded under similar excitation conditions in a 650-nm-thick Zeonex film, showing the occurrence of many different levels as well as on/off steps.

Results and Discussion

Fluorescence Transients. Typical fluorescence intensity trajectories (transients)—that is, fluorescence intensity of a single molecule as function of time—for **g0** and **g2** are shown in Figures 3 and 4, respectively (molecules embedded in a 30-nm thin PVB polymer film).

Sixty percent of the investigated transients for **g0** show a one-step photobleaching (Figure 3a), as can be expected for a single chromophore. In 35% of the transients, the fluorescence intensity drops to the background level (Figure 3b) for periods ranging from 5 to 1200 ms before irreversible photobleaching, an inevitable process in single-molecule spectroscopy, occurred. These drops in fluorescence intensity (one or two in a transient) are referred to as off times. Off times can originate from several processes. Often they are related to occupation of the triplet state.[44-46] As shown in the literature, a triplet lifetime can be

calculated from these off times if one presumes a simple three-level system consisting of the ground state, the first singlet excited state, and the first triplet excited state.[47] Fitting of the distributions of the off times of **g0**, taking into account this model, yields a triplet lifetime of 110 ms. This value is an upper limit as, due to the 5-ms bin time, off times shorter than the bin time will not be observed. Triplet lifetimes in the millisecond range were reported for other immobilized single molecules.[16,17,47-50] In 5% of the investigated transients, jumps between different emissive levels can be detected (Figure 3c). As will be elaborated further below, these jumps can be correlated to rotational diffusion of single model molecules in the polymer film.

Panels a and b of Figure 4 show transients for **g2** excited with linear polarized and circular polarized light, respectively. On/off behavior as well as jumps between different emissive levels can be detected for both excitation conditions.

The transients of **g2** show more levels and jumps and longer survival times (time of irradiation until irreversible photobleaching takes place) compared to those of the model under identical excitation conditions.[36] Transients of **g2** excited with linear polarized light (488 nm, 350 W/cm^2 at the sample) contain on average 7.9×10^5 detected photons (corrected for background noise) and survive on average 280 s before irreversible photobleaching occurs. Under similar excitation conditions, **g0** has an average survival time of 70 s and 1.5×10^5 detected photons (average of 84 molecules). Using circular polarized light at the same wavelength and the same excitation power leads for **g2** to transients containing on average 11×10^5 photons and showing a mean survival time of 450 s. The difference in the number of photons detected for the two excitation conditions can be rationalized by assuming that the average *z*-orientation of the sampled molecules is similar for the two excitation conditions. In the case of circular polarized excitation, all eight chromophores will be sampled, while in the case of linear polarized light, only a fraction of the eight chromophores will contribute to the absorption (see below). The longer survival times can be explained on the basis of sampling all chromophores versus addressing some of the chromophores. Long survival times always correspond with low levels at the end of the transient, as demonstrated in Figure 4b. In general, the highest levels are in the first part of the transient, whereas low levels are observed at the end of the transient. If the eight chromophores of **g2** absorbed and emitted independently of each other, one would expect mainly jumps between close-lying intensity levels. All of the fluorescence transients of **g2** show reversible jumps between a high level and a low level or the off level. Even the transients recorded using circular polarized light, exciting all eight chromophores in the dendrimer, show reversible jumps between the high level and the off level, as can be seen in the inset of Figure 4b. The duration of the off state for the reversible jumps (back to the initial intensity level) in the beginning of the transient varies from a few milliseconds

(44) Xie, X. S. *Acc. Chem. Res.* **1996**, *29*, 598−606.
(45) Xie, X. S.; Trautman, J. K. *Annu. Rev. Phys. Chem* **1998**, *49*, 441−480.
(46) Basché, T.; Moerner, W. E.; Orrit, M.; Wild, U. P. *Single Molecule Optical Detection, Imaging, and Spectroscopy*; Wiley VCH: Weinheim/Munich, 1997.
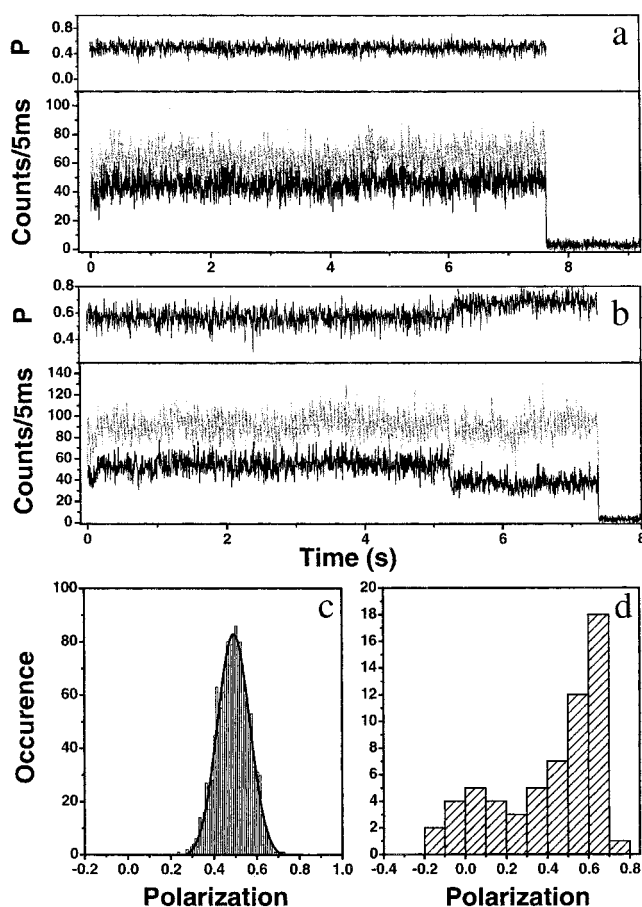(47) Yip, W. T.; Hu, D. H.; Yu, J.; VandenBout, D. A.; Barbara, P. F. *J. Phys. Chem. A* **1998**, *102*, 7564−7575.
(48) Weston, K. D.; Carson, P. J.; Metiu, H.; Buratto, S. K. *J. Chem. Phys.* **1998**, *109*, 7474−7485.
(49) Weston, K. D.; Carson, P. J.; DeAro, J. A.; Buratto, S. K. *Chem. Phys. Lett.* **1999**, *308*, 58−64.
(50) Ha, T.; Enderle, T.; Chemla, D. S.; Selvin, P. R.; Weiss, S. *Chem. Phys. Lett.* **1997**, *271*, 1−5.

to several hundreds of milliseconds. Off states in later parts of the transient can last for several seconds or tens of seconds. The eight chromophores being simultaneously in the off-state is an implausible explanation for the observed collective on/off behavior in the transients of **g2**. At this point, it must be emphasized that at the excitation powers used the formation of more than one singlet excited state at a time is very unlikely.[51] Another explanation could be that the eight chormophores are strongly coupled and hence act as one quantum system. If this system went to an off state, such as the triplet state, this would account for the collective phenomena observed for **g2**. No support can be found for this model from the solution data, as the absorption spectra of **g2** and **g0** hardly differ.[37] However, Coulombic interaction in the excited state is possible. Indeed, there is a difference in the fluorescence properties as expressed in the reduced quantum yield of fluorescence, the emission spectra, and the more complex time-dependent behavior.[37] Calculations show that all chromophores are well within the Föster radius for singlet energy transfer.[37] This implies that fluorescence will occur from the chromophoric site in the dendrimer that at a given point in the trajectory is lowest in energy and hence acts as a trapping site from which fluorescence will occur. From this, it can be deduced that off states have to be explained on the basis of radiationless deactivation channels that are opened via the energetically lowest chromophoric site. The nature of all deactivation channels in multichromophoric systems is, at the moment, not fully understood. For **g2**, the triplet state of the energetically lowest lying chromophoric site is one possible candidate. Excitation energy transfer from the first singlet excited state to the first triplet state resulting in the singlet ground state and a higher lying triplet state is a spin-allowed process.[52] It can occur in multichromophoric dendrimer systems such as **g2** if the rate constant of energy transfer from the singlet excited state to the triplet excited state is sufficiently high. The good overlap between the triplet absorption spectrum of **g2**, measured in solution via the transient absorption technique, and the emission spectra of both **g0** and **g2** in solution further supports this hypothesis.[53] The relaxation of the higher triplet state to the first triplet state is a very fast, spin-allowed nonradiative process. The competition between singlet/triplet energy transfer and fluorescence from S_1 might then account for the occurrence of both off levels and low levels within the binning time. A similar mechanism, involving singlet−triplet annihilation, was previously suggested in the literature to play a role in the multichromophoric allophycocyanin system.[26] As triplet lifetimes of several seconds are unlikely, other deactivation channels have to be considered. The formation of a radical/cation or radical/anion pair was suggested for a different multichromophoric system and might play a role in this system as well.[22,26,54] Part of the dynamics in the transients might arise from the different environments the single molecules can experience in the thin PVB film (glass/polymer interface, polymer, polymer/air interface as well as different functional regions in the PVB itself). Therefore, in addition **g2** was studied in 650-nm-thick films of the structurally more uniform aliphatic polymer Zeonex (polynorbornene). As displayed in panel c of Figure 4, collective on/off jumps and different emission levels are observed in transients of single **g2** molecules under identical

(51) Eggeling, C.; Widengren, J.; Rigler, R.; Seidel, C. A. M. *Anal. Chem.* **1998**, *70*, 2651−2659.

(52) Barltop, J. A.; Coyle, J. D. *Excited states in organic chemistry*; John Wiley & Sons: New York, 1975.

(53) Lor, M., licentiaatsthesis, University of Leuven, 1999.

(54) Hu, D. H.; Yu, J.; Barbara, P. F. *J. Am. Chem. Soc.* **1999**, *121*, 6936−6937.

Figure 5. Typical examples of parallel (‖)- and perpendicular (⊥)-polarized transients of **g0**. (a) ‖- and ⊥-polarized transient trace as well as a polarization (*p*) trace (see text) for **g0**. A *G*-factor of 0.37, accounting for differences in detection sensitivity for both polarizations in the setup, has been used in the calculation of *p*. The *p*-trace shows no discrete jumps but varies due to the noise on the detected signal. (b) Five percent of the **g0** molecules show jumps in intensity that can be seen in the *p*-trajectory as well. (c) Histogram and Gaussian fit of the *p*-values of the molecule depicted in (a). (d) Histogram of the *p*-values for 80 molecules of **g0**, showing the photoselection with linear polarized excitation light.

excitation conditions. This clearly shows that dynamics are inherent to the multichromophoric system.

Polarized Fluorescence Transients. (a) Linear Excitation. Figure 5a depicts a fluorescence transient acquired for a single molecule with the detection conditions such that the emitted light was split in its parallel-polarized and perpendicular-polarized components (with respect to the polarization of the excitation light) and detected with two independent detectors. The parallel- and perpendicular-polarized components are shown in gray and black, respectively. The polarization *p* was calculated according to eq 1 from the signals in both detectors. $I_{\parallel}$ is the

$$p = \frac{I_{\parallel} - GI_{\perp}}{I_{\parallel} + GI_{\perp}} \qquad (1)$$

intensity of fluorescence with the polarization parallel to the excitation light, $I_{\perp}$ is the intensity of emitted light perpendicular to the excitation light, and *G* is a correction factor that accounts for the difference in sensitivity for the detection of emission in the perpendicular and parallel channels. At this point it must be noted that the use of high numerical objective lenses causes an additional depolarization that should be taken into account.[55] In a recent paper, Ha et al.[56] showed that the deviation for *r*,

the anisotropy, is less than 10% when properly focused on a single molecule. Since this is comparable to the broadening of r and p distributions induced by shot noise, no additional correction was done. For an immobilized single-chromophore, single-molecular system, the value of p can range from 1 to -1. A value of 1 corresponds to a case where the transition dipole is perfectly parallel with the orientation of the linear polarized light, while a value of -1 corresponds to a case where both are perpendicular. This and similar excitation/detection schemes allow the determination of the orientation of the component of the transition dipole moment in the $x-y$ plane (and eventually also the z-component), as demonstrated in a number of recent publications.[9,57-63]

A typical polarized fluorescence transient for **g0** is shown in Figure 5a. The corresponding polarization (p) trajectory shows only shot-noise-induced variations. When the values in the p-trajectory of a single molecule are histogrammed, they can be fitted with a single Gaussian distribution (Figure 5c). For the molecule shown here, a Gaussian distribution centered around 0.49 with a width of 0.15 was found. The width of the Gaussian distribution depends on the detection intensity in the two channels and varies between 0.10 (sum of detected counts in the 2 channels (Σ) >150 counts/5 ms) and 0.25 (Σ < 40 counts/5 ms). As mentioned above, different intensity levels could be observed in only 5% of the transients (Figure 5b). The different levels can be seen also in the corresponding p-trajectories and point toward a reorientation of the transition dipole moment of the molecule in the polymer film. From the p-trajectory in Figure 5b, a rotation of 10° in the $x-y$ plane was calculated. It is interesting to note that, upon excitation with polarized light, the distribution of calculated p-values over a large number of single molecules is biased toward values close to $+1$, showing the photoselection resulting from exciting single molecules with linear polarized light (Figure 5d).

The behavior of **g2** is again much more complicated. Discrete jumps in the p-trajectory are observed for every molecule studied. Two representative examples are shown in Figure 6a and b. Upon inspecting the transients in Figure 6a, one observes numerous intensity jumps that are not necessarily correlated with p-jumps. After the first off-level (approximately 1 s), the contributions of the emitted photons in the two detectors recover the original level, and hence no change in p is seen. This means that the emitting chromophoric site is still the same or one with an identical orientation. After 3 s, an intensity jump occurs in the transient. This jump does not give rise to a change in the relative contribution of $I_{\parallel}$ and $I_{\perp}$ as p does not change. A likely interpretation is that one chromophore formerly contributing to the fluorescence via absorption and energy transfer was photobleached. Another explanation is the reorientation of one or more chromophores while the emitting one keeps its orientation. A second on/off jump after 7 s results in a change in the relative contributions and, as a consequence, in a change in p. In contrast
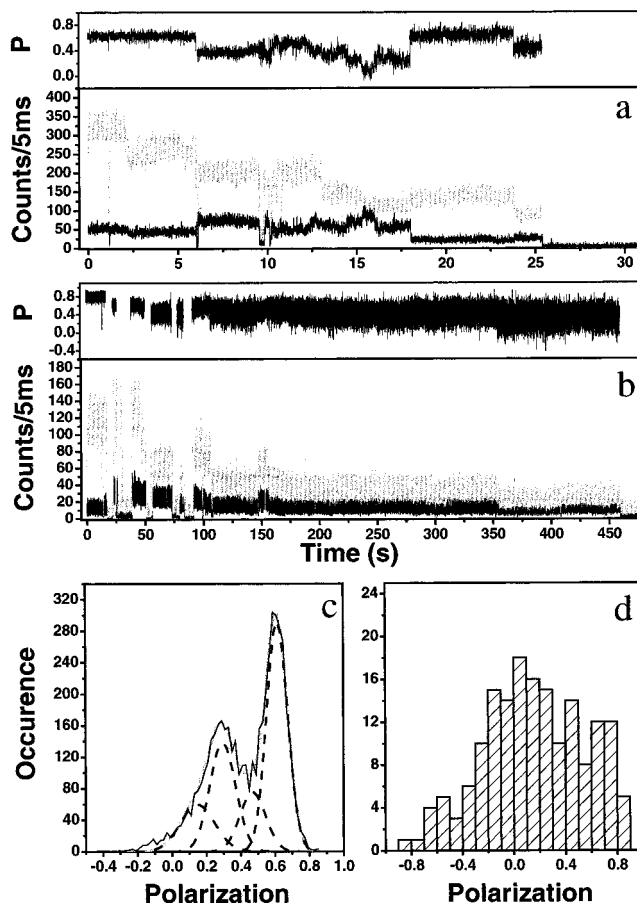
Figure 6. (a, b) Two examples of ∥- and ⊥-polarized fluorescence transients for **g2**. Particular in (a) is that the value for p returns to the start value at the end of the transient. The p-trajectory in (b) shows a stepwise change from a p-value of 0.8 to a value of 0. (c) Histogram of the p-trajectory in (a) (black line) and the corresponding fit (gray line). The histogram needs four Gaussian distributions (dotted lines) for a satisfactory fit. Constraints were put on the widths of the Gaussians according to the values found for different intensity levels for the model compound. The following p-values for the different distributions were recovered: 0.15, $w = 0.2$; 0.23, $w = 0.15$; 0.47, $w = 0.15$; 0.61, $w = 0.12$. (d) Distribution of all the p-values calculated from 64 transients of **g2**.

to the first jump, this can be explained with a different chromophoric site emitting or with a reorientation of the initial emitting chromophoric site. The molecule enters a period of more frequent small changes after a third on/off jump (11 s). At lower levels, the relative contributions become noisier. After 16 s, the contribution is equal in both channels for a short period. After 19 s, the relative contributions are exactly the same as the initial values, although the overall intensity is lower by a factor 3−4. A histogram of the values in the polarization trajectory is shown in Figure 6c. The histogram could be fitted satisfactorily with four Gaussian distributions, resulting in p values of 0.61, 0.47, 0.23, and 0.15. Appropriate constraints were set for the width of the Gaussians according to the earlier mentioned values of the Gaussian width found for **g0**. On average, 3−4 distinctly different p-values are found in the time interval of a transient. The jumps in p are in good agreement with the model in which emission is assumed to occur from one chromoporic site only. When this chromophoric site photobleaches, the emission will occur from a new lowest energetic chromophoric site. This will result in a different p-value if the new emitting chromophoric site has a different orientation as the previous one. In view of this model it is

(55) Koshioka, M.; Sasaki, K.; Masuhara, H. *Appl. Spectrosc.* **1995**, *49*, 224−228.

(56) Ha, T.; Laurence, T. A.; Chemla, D. S.; Weiss, S. *J. Phys. Chem. B* **1999**, *103*, 6839−6850.

(57) Bartko, A. P.; Dickson, R. M. *J. Phys. Chem. B* **1999**, *103*, 11237−11241.

(58) Bartko, A. P.; Dickson, R. M. *J. Phys. Chem. B* **1999**, *103*, 3053−3056.

(59) Empedocles, S. A.; Neuhauser, R.; Bawendi, M. G. *Nature* **1999**, *399*, 126−130.

(60) Ruiter, A. G. T.; Veerman, J. A.; GarciaParajo, M. F.; vanHulst, N. F. *J. Phys. Chem. A* **1997**, *101*, 7318−7323.

(61) Betzig, E.; Chichester, R. J. *Science* **1993**, *262*, 1422−1425.

(62) Trautman, J. K.; Macklin, J. J. *Chem. Phys.* **1996**, *205*, 221−229.

(63) Macklin, J. J.; Trautman, J. K.; Harris, T. D.; Brus, L. E. *Science* **1996**, *272*, 255−258.

surprising to see that at the end of the transient *p* recovers exactly to the same value as at the start of the transient. This can be rationalized by assuming that the initial emitting chromophoric site was not permanently photobleached. Another, more probable explanation can be given if one considers the structure of the molecule.

In the simplest approximation, the projection of the transition dipoles of the chromophores at the rim of a dendrimer in the $x-y$ plane results in eight equidistant transition dipoles. Assuming an absence of reorientations or interactions among the chromophores besides energy transfer to one of the chromophores, a maximum of four *p*-values ranging from -1 to 1 should be found as the transition dipoles show a 4-fold symmetry with respect to the detectors. Although in reality this simple model does not hold, it helps to understand why certain *p*-values can be found several times within one trajectory. Figure 6b shows a molecule where *p*, as a function of time, shows a stepwise change from a high value toward a value close to zero. Also in this example, four different values for *p* were found, but the recovery to the initial *p*-value was not seen.

Assuming the emission to occur from one chromoporic site, *p* should have a broad distribution around zero, since the transition dipole of the chromophore can adopt all orientations between parallel and perpendicular. Values for *p* ranging from -0.8 to 0.8 were encountered for different transients of **g2**. When all *p*-values of the different trajectories are histogrammed, a broad distribution is observed (Figure 6d).

(b) Modulated Excitation. A similar experiment was performed by imposing a 3.3-Hz modulation frequency on the linear polarized light used. When a similar excitation scheme is used for immobilized single-chromophore single molecules, such as model compound **g0**, the fluorescence intensity follows the excitation modulation and drops to the background level whenever the exciting light and of the transition dipole moment are perpendicular with respect to each other. A fluorescence intensity trace for **g0**, exemplifying the modulation and the drop of the fluorescence intensity to the background level, is shown in Figure 7.

For the multichromophore system it cannot be expected that the modulated fluorescence intensity drops to the background level in the same way as for the model compound, as the different chromophores have different orientations. Therefore, at any time, some of them can be excited unless their transition dipole moment is perfectly parallel to the *z*-axis of the setup. A typical example of a modulated transient is shown in Figure 8. Panels b and c are enlarged parts of the transient at the times indicated. The first part of the transient shows, besides increased fluctuations in intensity in the two detection channels, the same features as the transients shown above. Several on/off jumps can be seen. The increased intensity fluctuations have a certain periodicity, apparently with a frequency faster than the imposed 3.3-Hz frequency. After 12 s, the molecule goes to a long off state. At $t = 50$ s, the molecule starts to emit again at a lower level. The relative contribution of the fluorescence in the two detectors clearly changed. Modulation in the fluorescence intensity can be seen but not with the imposed modulation frequency. Furthermore, in neither of the channels does the intensity drop to the background level. Only at around 92 s, after several jumps in intensity and relative contributions in the two channels, finally deep modulation with the imposed frequency is found again. This clearly proves that, during this period, only one chromophore absorbs and emits. To understand the modulation patterns in the early part of the transient, modeling was performed. The frequency and the depth of
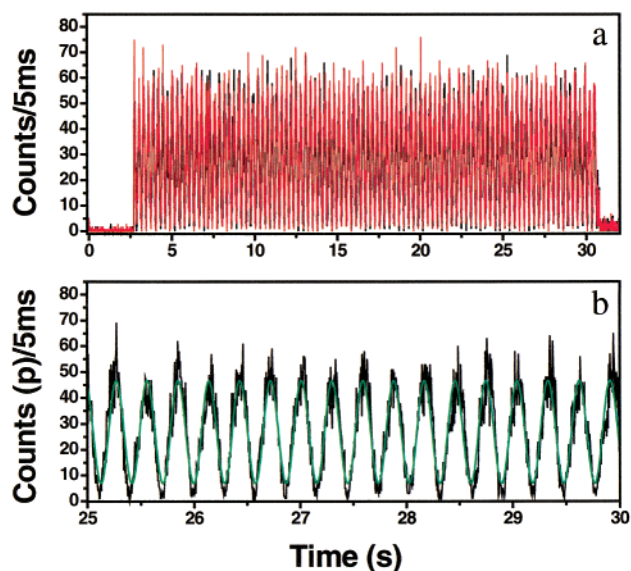

Figure 7. (a) Modulated transient trace for a **g0** molecule (excitation at 488 nm, 500 W/cm^2). The modulation frequency was 3.3 Hz. Parallel- and perpendicular-polarized components were recorded in different detection channels (black for parallel-polarized light, red for perpendicular-polarized light, signals corrected with the *G*-factor of the setup). The intensity in both channels follows the imposed modulation. Note that the intensity drops to the background level when the orientation of the transition dipole moment of the chromophore is perpendicular to the orientation of the linear polarized light (b). The intensity traces could be perfectly fitted with a cosine function (green curve in (b); only the results for parallel-polarized light are shown). For this case, the intensities in the two channels are similar. From this, an angle of 45° for the orientation of the transition dipole moment in the $x-y$ plane can be calculated.
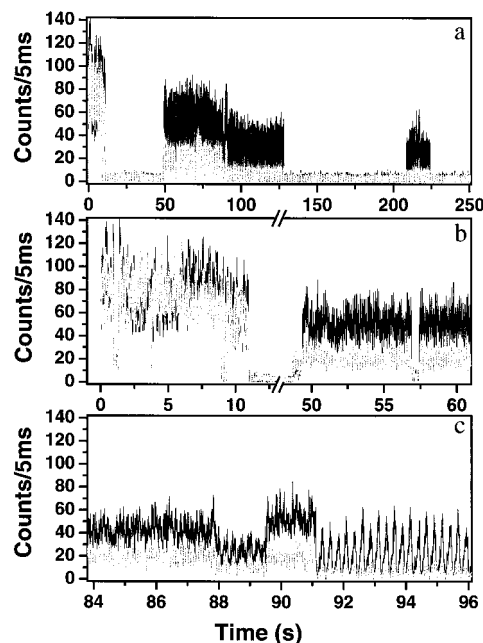
Figure 8. (a) Modulated transient trace for a **g2** molecule (excitation at 488 nm, 500 W/cm^2, parallel-polarized light given in black, perpendicular-polarized light in gray). (b, c) Zooms in different regions of the transient. Deep modulation to the background level can be seen only in the last part of the transient, indicating that at that moment only one chromophore is still absorbing and emitting.

modulation are directly related to the number of differently oriented chromophores in the molecule. Details on the modeling results will be published elsewhere.
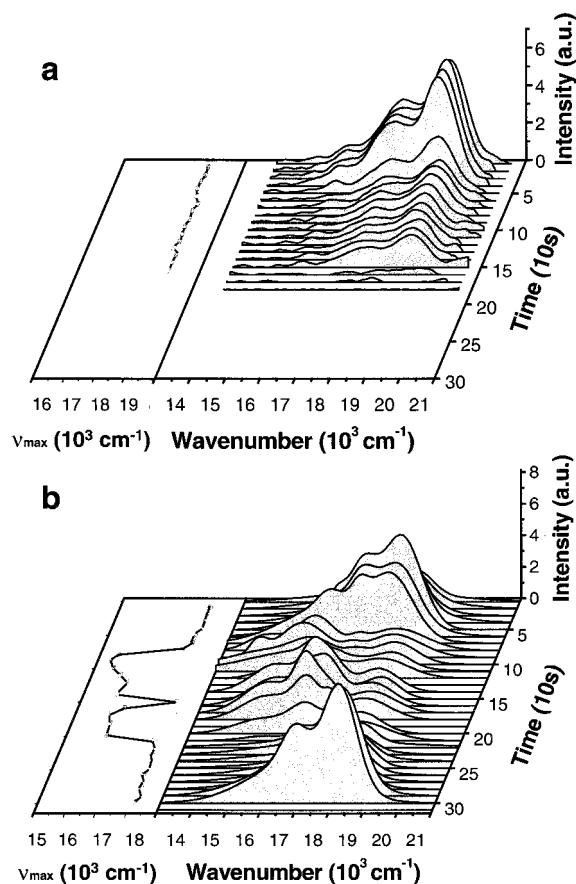
Figure 9. Spectral runs of **g0** (a) and **g2** (b) in a thin PVB film excited at 488 nm (intensity of 350 W/cm²). Consecutive spectra were taken (integration time per spectrum of 10 s) until irreversible photobleaching occurred. Spectra were corrected, and the fitted data are shown. The left figures are the trajectories as a function of time of the emission maximum of the corresponding spectra.

Emission Spectra. The spectra of single molecules of **g0** show a uniform spectral shape with a vibrational fine structure similar to the solution spectra and only small changes in emission maxima, as shown in Figure 9a. Individual molecules of **g2** behave completely differently. Figure 9b depicts a series of spectra as function of time (spectral run) from a single dendrimer molecule showing a complex and dynamic spectral behavior. On the left side of the figure, a trajectory of the emission maximum of the single dendrimer molecule is depicted. Changes in the emission maximum as large as 3000 cm⁻¹ are observed, whereas the trajectory of the model compound shows changes only up to 200 cm⁻¹.

As can be seen in Figure 9, not only do large spectral jumps occur, but also the shape of the spectra can differ from frame to frame. The spectral shape ranges from a fine structure similar to the spectrum of the model compound in solution (Figure 10a) to a spectrum consisting of a broad unstructured band (Figure 10c). Also, spectra with apparently three or four bands can be seen (Figure 10b). Transitions between the different spectral shapes could be observed within one spectral run of a single molecule.

These observations support the model, based on ensemble measurements (Figure 2), that indicates that the chromophore distribution at the rim of the dendrimer is not homogeneous in space but also contains regions where chromophores are either in close contact or interacting in the ground state. Spectra showing fine structures are attributed to emission from isolated chromophores, whereas the unstructured spectra are attributed
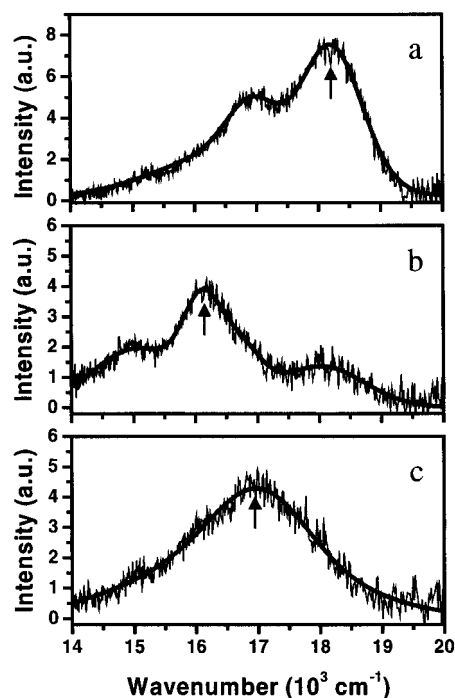
Figure 10. Different spectral shapes that can be observed for **g2** (both original data and fitted data are shown). (a) Spectrum with fine structure, similar to that of the model compound in solution ($\lambda_{max} = 18\ 200$ cm⁻¹). This spectrum is attributed to isolated chromophores in the dendrimer. (b) Spectrum with additional structure never observed in solution. (c) Broad, unstructured, and red-shifted spectrum ($\lambda_{max} = 16\ 900$ cm⁻¹) attributed to interacting chromophores within one dendrimer molecule.

to emission from dimer-like interacting chromophores. As a result of this interaction, the emission maximum is red-shifted. This can be seen when one compares the distribution of emission maxima in Figure 11. The distribution for **g2** (excitation at 488 nm, 1961 spectra) is clearly broader than the distribution for **g0** (excitation at 488 nm, 753 spectra). The broadening is most prominent at the low-wavenumber side of the distribution (filled bars), resulting in a red-shifted average of the distribution.

Transitions from unstructured spectra to structured spectra are observed and can be explained by taking into account that, while most or all of the chromophores, depending on orientation and polarization of the exciting light, contribute to the absorption of photons, emission will occur from the energetically lowest lying chromophoric site due to energy transfer. As demonstrated with the transients, when this chromophoric site photobleaches,[64] or when a different chromophoric site due to changes of the local environment gets lower in energy, emission will occur from the new lowest energetic chromophoric site. The fact that spectra are found with three or four vibrational bands indicates that, during the collection time of a spectrum (10 s), two different chromophores with two distinct energy maxima contributed to the emission. From this it follows that spectral broadening or loss of fine structure can also occur as a result of spectral jumps between chromophoric sites that are close in energy.

To validate the assumptions stated above, spectral runs were recorded for 50 individual molecules with excitation at 488 and 543 nm. In Figure 12, the emission maximum from the first 10

(64) A first step in the photooxidation process might be the formation of an endoperoxide as recently proposed for the terrylene chromophore, Basché, T. *Molecular Processes in small time and space domains*; Presented at the 8th JST international symposium, 2000 (abstract).
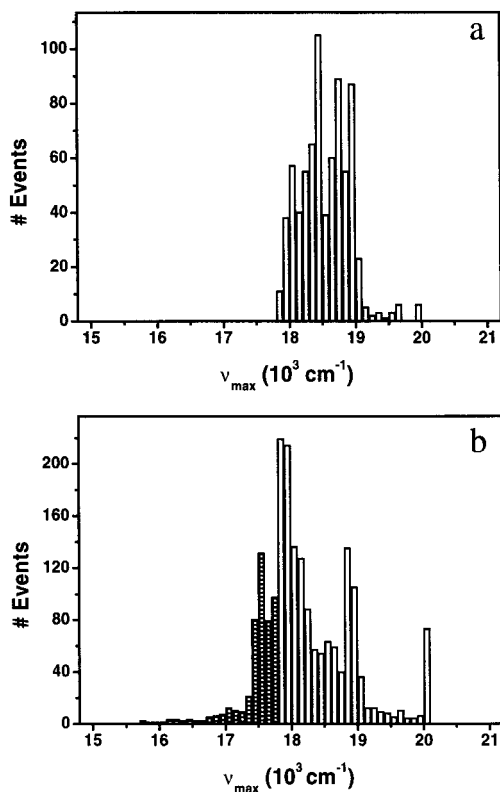
Figure 11. Distributions of λ_{max} of spectra recorded for **g0** (a) and **g2** (b) (excitation at 488 nm, intensity 350 W/cm^2). The distributions contain respectively 753 and 1961 spectra.
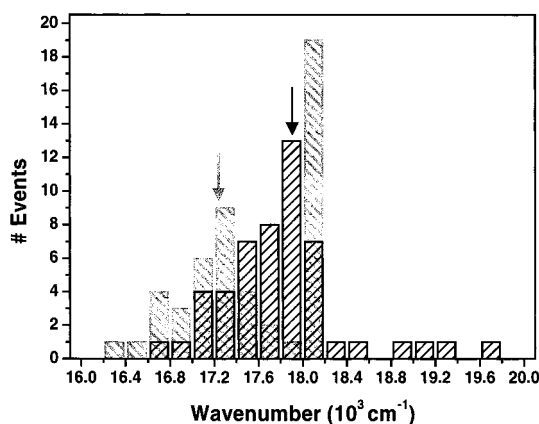
Figure 12. Distributions of λ_{max} of spectra recorded for **g2** excited at 488 nm (black bars, intensity of 300 W/cm^2) and 543 nm (gray bars, intensity of 700 W/cm^2). At each wavelength of excitation, 50 molecules were investigated. Only the first spectrum of each spectral run (10 s of irradiation) is shown in these distributions. The black and the gray arrows indicate the mean value of the distributions at 488 and 543 nm, respectively. The high gray bar centered at 18 100 cm^{-1} is due to cutoff of the dichroic mirror used.
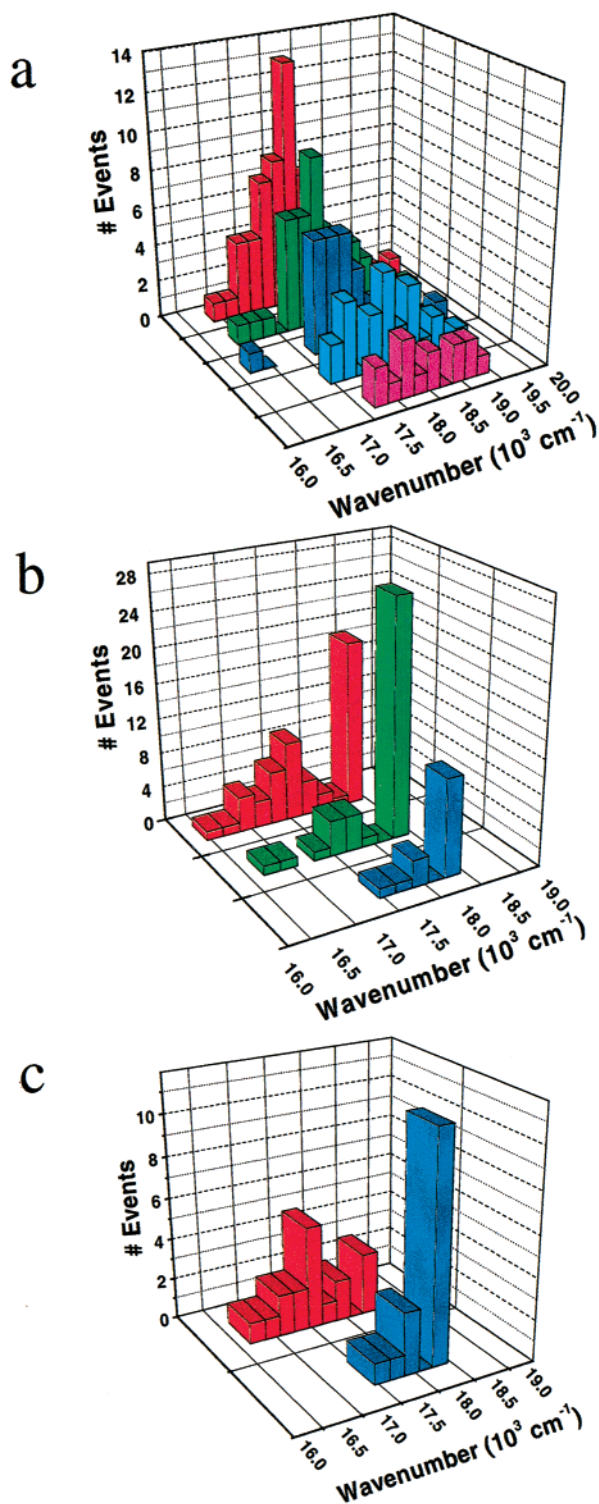
s is shown. Excitation at 543 nm results in a higher probability of a red-shifted emission of the initial spectrum compared to excitation at 488 nm. This observation fits in the proposed solution model. As the dimer-like interacting chromophores should absorb and emit at longer wavelength compared with the isolated chromophores, direct excitation of the interacting chromophores (543 nm) should result in a higher probability for the red-shifted emission. Figure 12 shows that the average emission maximum upon excitation at 543 nm, where direct excitation of the dimer-like entity is more likely, is shifted 1000 cm^{-1} compared to that upon excitation at 488 nm.

As can be seen in Figure 13, for both excitation wavelengths it is observed that the emission maximum gradually shifts to higher energies. Figure 13a shows the distribution of the emission maximum of the spectra of 50 single molecules excited at 488 nm as a function of time, whereas Figure 13b shows the evolution of the distribution for excitation at 543 nm. From the distributions in Figure 13, it can be seen that with time the emission maximum shifts to higher energy and that the number of molecules contributing to the distribution decreases. This suggests that photobleaching of low-energy chromophoric sites occurs. This furthermore supports the idea stated before, that bleaching occurs in a stepwise fashion within one single molecule and that the bleached form is not a quencher for the excited perylenecarboximide.
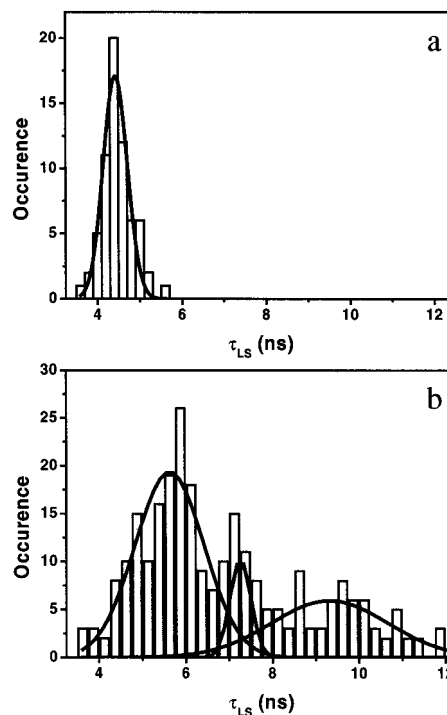
One could argue that red-emitting chromophoric sites bleach faster than the blue-emitting form, to explain this shift of the maxima to higher energies. In Figure 13c, the distributions of the emission maxima of the initial spectra of the molecules contributing to the distribution after 200 s in Figure 13b are shown. The data indicate that selective photobleaching can be ruled out as a reason for the observed shift toward higher energy.

Time-Resolved Measurements. Fluorescence decays as a function of time (decay run) of single molecules were recorded for both **g0** and **g2** at excitation wavelengths of 488 and 543 nm. The decays for each single molecule were analyzed by linking instrument response function (irf), scatter, and time shift over all the recorded decay traces within the decay run. The decays were analyzed using the least-squares (LS) method. It was recently shown that for approximately 100 counts in the maximum, the decay parameters obtained with the LS method differ only 5% from the parameters obtained with the maximum likelihood estimator (MLE) method (for monoexponential decays).[42] The distributions of the decay times for **g0** (38 molecules analyzed, 66 decay times) and **g2** (41 molecules analyzed, 261 decay times) are shown in Figure 14 (excitation occurred at 543 nm). For all decays of **g0**, good fit parameters were obtained when the decays were monoexponentially fitted. The decay times obtained this way for **g0** show a Gaussian distribution centered around a value of 4.4 ns. This value is in good agreement with the decay time found in solution ($\sim$4 ns) for **g0**.[37]

The distribution of decay times for **g2** is clearly much broader, with a pronounced tail at long decay times (Figure 14b). At least three Gaussians are needed to fit the distribution, resulting in values of around 5.5 and 9.5 ns, and a small contribution of an intermediate decay time of 7 ns. The short and long decay values resemble the values found in solution for **g2** ($\sim$4 and $\sim$8 ns).[37] The difference in the decay times between solution and immobilized single molecules might reflect a difference in conformational dynamics. When excited at 488 nm, 40% of the investigated molecules show a long decay component at some point of their decay time trajectory. When the molecules are excited at 543 nm, this number rises to 60%. Upon excitation at 488 nm, the long decay time is only found immediately after the start of the irradiation. Decay trajectories that show solely the long decay time are only observed for excitation at 543 nm. From solution measurements, it is also known that the contribution of the 8-ns decay component increases in decays recorded at the long-wavelength side of the emission band. The long decay time is therefore attributed to emission from the dimer-like interacting chromophoric sites. The pronounced presence of the long decay time at 543 nm is the result of direct excitation into the dimer-like interacting chromophoric sites at that wavelength. The intermediate decay could be the result of both
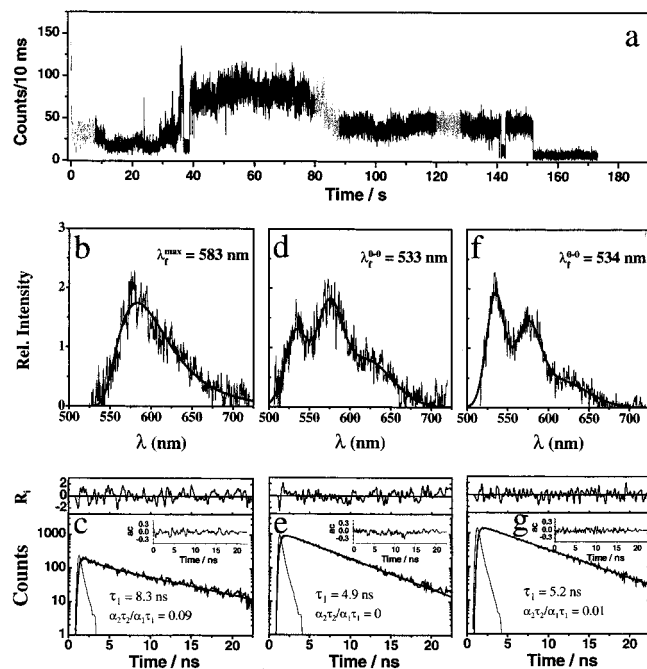
Figure 14. Decay time distributions for 38 **g0** molecules (a) and 41 **g2** molecules (b) (excitation at 543 nm). Whereas the distribution for **g0** can be fitted with a narrow Gaussian, yielding an average value of 4.4 ns, the distribution for **g2** is much broader, with a pronounced tail at long decay times. At least three Gaussians are needed to fit the distribution. The three corresponding average values are 5.5, 7, and 9.5 ns (see text).

isolated and interacting chromophoric sites emitting during the recording of the decay. Simulations indeed show that a two-exponential decay (similar contributions of a 5- and and 8-ns component) with slightly more than 100 counts in the maximum can be equally well fitted with a single exponential, yielding an intermediate decay time. Due to the limited time resolution of the setup (720-ps response time of the detectors) and the low amount of data points, the very fast component measured in the ensemble cannot be observed at the single-molecule level. Nevertheless, in about 40% of the **g2** molecules, it is necessary to add a second short component (∼1 ns) when analyzing the decays in order to get a satisfactory fit.

Combined Time-Resolved Measurements, Spectra, and Transients. As shown above, single-molecule spectroscopy of the dendrimer makes it possible to observe spectra and decay times that were attributed to isolated chromophoric sites as well as spectral and temporal behavior that was linked with dimer-like interacting chromophoric sites. Recording both temporal and spectral parameters simultaneously for a single molecule would then make it possible to prove irrevocably the assignments mentioned above. Simultaneous measurements were performed by placing a hybrid beam splitter cube in the detection path, guiding equal amounts of emitted photons to the camera and APD detector, respectively (excitation occurred at 488 nm). Only few examples of combined spectral and time-resolved measurements at room temperature have been reported in the literature.[62,63]

The transients, spectra, and decays were recorded with 10 ms, 8 s, and 2 s of integration time, respectively. The gray parts of the transient depicted in Figure 15a correspond to the spectra and decays shown in panels b–g of Figure 15. The first spectrum (b, 0–8 s) is unstructured and has its maximum at 583 nm. Analyzing the corresponding summed-up decays (4,

Figure 13. Spectral distributions as a function of time, excited at 488 nm (a, 300 W/cm²) and 543 nm (b, 700 W/cm²). The distributions have a color code that corresponds to the applied irradiation time (integration time for each spectrum, 10 s): red = 10 s, green = 100 s, blue = 200 s, turquoise = 300 s, pink = 400 s. (a, b) The centers of mass of the distributions, at both 488 and 543 nm of excitation, show a blue shift as a function of time. Due to photobleaching, the number of spectra taken into account in a distribution at a later times decreases. As the excitation intensity at 543 nm is more than double that at 488 nm, the photobleaching is more pronounced at the former excitation wavelength. (c) The red distribution corresponds to the initial spectra of the molecules that still showed fluorescence after 200 s of irradiation (blue distribution in (b)).

Figure 15. Combined and simultaneous transient, spectral, and time-resolved fluorescence decay measurements on a single **g2** molecule (excitation at 488 nm, 650 W/cm^2). (a) Transient recorded with 10-ms binning time. The regions that correspond to the further discussed spectra and decays are colored in gray. (b, c) Spectrum and decay corresponding to the first gray region in the transient. Integration time for the spectrum is 8 s. The four decays recorded during this time were summed to one decay and analyzed. The spectrum is clearly unstructured, with a maximum at 583 nm. The decay is two-exponential with a long decay component of 8.3 ns. (d, e) Spectrum and decay corresponding to the second gray region. The decay of 4.9 ns corresponds to a structured spectrum with distorted vibronic features. (g, f) Spectrum and decay corresponding to the third gray region in the transient. The spectrum corresponds to a solution spectrum of **g0**, and a decay time of 5.2 ns was obtained from the corresponding decay.

c) resulted in a decay time of 8.3 ns. This decay is not monoexponential. A second short component, analyzed as 1 ns, contributes roughly 10% to the decay. This short decay component is associated with the excitation delocalization processes in the dendrimer, leading here to dimer-like emission. The third spectrum (f, 120–128 s) is clearly structured and resembles very well a solution spectrum of **g0**. A decay time of 5.2 ns is found for the decay (g) corresponding to this spectrum, as well as a contribution of 1% of the short component. All the decays associated with structured spectra similar to the spectrum of **g0** had a decay time of around 5 ns. During the recording of the second spectrum (d, 80–88 s), a clear jump in the transient can be observed. The spectrum shows three bands with distorted vibrational contributions. As explained before, this could be due to two different isolated chromophoric sites emitting during the collection of the spectrum. The corresponding decay (e) could be fitted with a decay time of 4.9 ns. In this case, no short component was needed to get a satisfactory fit. Sometimes, apparently unstructured spectra also correlate with a decay time of 5–6 ns. As explained before, an unstructured spectrum can originate from two or more closely overlapping structured spectra and not from dimer-like interacting chromophores within one molecule.

The combined and simultaneously recorded spectra and decays at the single-molecule level incontestably prove the proposed model that links a short/long decay time and structured/unstructured spectrum to isolated chromphores and dimer-like interacting chromophores, respectively.

Conclusions

In this contribution, a multichromophoric dendrimer system containing eight chromophores at the rim was investigated at the single-molecule level. Fluorescence intensity traces, polarized fluorescence intensity traces, spectral runs, decay runs, and combinations thereof were recorded for a large number of individual molecules. These data were compared with similar sets of data obtained for the model compound **g0**. Excitation delocalization as well as emission from a dimer-like entity, which might be already present at the ground state, could be observed at the single-molecule level. Combination of decay runs and spectral runs could clearly link the long decay time of 9 ns with this dimer-like entity. This clearly establishes single-molecule spectroscopy, besides being an interesting and emerging field of spectroscopic investigations,[65] as an important investigative tool in the whole of spectroscopic techniques.

One of the most interesting findings of this study is the presence of collective or cooperative effects in the dendritic system. Collective or cooperative effects are known to occur in strongly coupled systems such as *J*-aggregates, antenna systems of bacteria, and conjugated polymers. These effects are related to the processes of energy transfer and exciton coupling. The observation of collective on/off jumps of all eight nonconjugated and only weakly interacting chromophores is rather unexpected. One possible mechanism leading to this behavior is singlet–triplet energy transfer in the multichromophoric system. All the previously presented data suggest structural inhomogeniety at the single-molecule level leading to complex temporal behavior, in part accentuated by the stepwise photobleaching of the multichromophoric system.

Dendrimer synthesis using a shape-persistent core makes it possible to get a well-defined number of chromophores in a confined space. This approach makes it possible to gain control over distances among chromophores and their relative orientation, and hence over the extent of their interactions. Whereas the present system still has flexibility around the central biphenyl bond leading to possible conformational distributions, more stringent control could be obtained with a central sp^3 core carbon. Studies on such systems are presently underway. It can be envisioned that these and similar studies will deepen the understanding of fundamental photophysical processes occurring in all kinds of multichromophoric systems.

(65) Tamarat, P.; Maali, A.; Lounis, B.; Orrit, M. *J. Phys. Chem. A* **2000**, *104*, 1–16.